

Modeling Angular-Momentum History in Dark-Matter Halos

Ariyeh H. Maller, Avishai Dekel

Racah Institute for Physics, The Hebrew University, Jerusalem 91904, Israel

and

Rachel S. Somerville

Institute of Astronomy, Madingley Road, Cambridge CB3 0HA, UK

ABSTRACT

We model the acquisition of spin by dark-matter halos in semi-analytic merger trees. We explore two different algorithms; one in which halo spin is acquired from the orbital angular momentum of merging satellites, and another in which halo spin is gained via tidal torquing on shells of material while still in the linear regime. We find that both scenarios produce the characteristic spin distribution of halos found in N-body simulations, namely, a log-normal distribution with mean ≈ 0.04 and standard deviation ≈ 0.5 in the log. A perfect match requires fine-tuning of two free parameters. Both algorithms also reproduce the general insensitivity of the spin distribution to halo mass, redshift and cosmology seen in N-body simulations. The spin distribution can be made strictly constant by physically motivated scalings of the free parameters. In addition, both schemes predict that halos which have had recent major mergers have systematically larger spin values. These algorithms can be implemented within semi-analytic models of galaxy formation based on merger trees. They yield detailed predictions of galaxy properties that strongly depend on angular momentum (such as size and surface brightness) as a function of merger history and environment.

Subject headings: galaxies:formation—galaxies:spiral

1. Introduction

Understanding the origin of spin in rotationally supported disk galaxies is clearly a crucial part of any theory of galaxy formation (Hoyle 1951). The general theory (Fall & Efstathiou 1980) reproduces galactic disks with roughly correct sizes, based on the assumptions that the gas originally had the same specific angular momentum as dark-matter (DM) halos do today, and that the infalling gas conserves specific angular momentum (Mestel 1963).

The origin of angular momentum in dark-matter halos can be understood in terms of linear tidal torque theory in which protohalos are torqued by the surrounding shear field (Hoyle 1951; Peebles 1969; Doroshkevich 1970; White 1984; Barnes & Efstathiou 1987; Steinmetz &

Bartelmann 1995; Porciani, Dekel, & Hoffman 2001b). Many models for the formation of galactic disks have been proposed based on the general picture of Fall & Efstathiou. Some of these models construct disk galaxies solely from the properties of the final halos (Blumenthal et al. 1986; Flores et al. 1993; Dalcanton, Spergel, & Summers 1997; Mo, Mao, & White 1998; van den Bosch 2000), and others incorporate the mass-accretion histories of the halos (White & Frenk 1991; Kauffmann, White, & Guiderdoni 1993; Cole et al. 1994, 2000; Kauffmann 1996; Avila-Reese, Firmani, & Hernández 1998; Firmani & Avila-Reese 2000; Somerville & Primack 1999; Somerville, Primack, & Faber 2001).

The halo spin is a crucial element for modeling important physical quantities such as galactic-disk size, surface brightness, star formation rate, and

rotation velocity in semi-analytic models. However, in none of the previous models is the angular momentum of DM halos assigned self-consistently based on their mass accretion and merger histories, primarily because an appropriate simple recipe for this buildup of spin has not yet been developed. The aim of this paper is to provide such a recipe.

We explore two scenarios. In the first, halo spin is generated by the transfer of orbital angular momentum from satellites that merge with the halo (orbital-merger scenario). This scenario was suggested by Vitvitska et al. (2001), who also compare it with simulations in more detail than is done here. In the second, linear tidal-torque theory is applied to spherical shells of infalling matter (tidal-torque scenario). Each recipe is applied in turn, within Monte Carlo realizations of halo merger histories generated using the extended Press-Schechter approximation and the method of Somerville & Kolatt (1999). We test and calibrate these scenarios by comparing their predictions for the distribution of spin with the known results of N-body simulations.

The outline of the paper is as follows. Section 2 presents our notation and defines the quantities of interest. Section 3 explores the orbital-merger scenario, while Section 4 addresses the tidal-torque picture. In § 5 we discuss the dependence of the spin distribution on mass, cosmology and redshift. In § 6 we study the dependence of the spin distribution on halo merger history. In § 7 we conclude and provide a brief discussion concerning the implications for disk sizes.

2. Background

The angular momentum of a halo, J , is commonly expressed in terms of the dimensionless spin parameter (Peebles 1969)

$$\lambda = J\sqrt{|E|}/GM^{5/2}, \quad (1)$$

where E is the internal energy of the halo. In practice, the computation or measurement of this quantity, especially the energy, may be ambiguous. Furthermore, it introduces an undesired dependence on the specifics of the halo density profile, which depends on cosmology, redshift and halo mass (see Bullock et al. 2001) and may also depend on merging history (Wechsler et al. 2001b).

Instead, following Bullock et al. (2000a), we will focus on the distribution of the variable

$$\lambda' = \frac{J}{\sqrt{2}MV_{\text{vir}}R_{\text{vir}}}, \quad (2)$$

which is more straightforward to compute and does not explicitly depend on the density profile of the halo. For a singular isothermal sphere truncated at a radius R_{vir} , this parameter is equal to the traditional spin parameter, $\lambda' = \lambda$. They are also approximately equal for halos with a more realistic density profile: an NFW profile (Navarro et al. 1996) with concentration $c_{\text{vir}} \approx 10$.

Many studies based on N-body simulations have revealed that the distribution of spin parameter λ is well fit by a log-normal distribution, and varies very little as a function of halo mass, redshift, or cosmological model. Bullock et al. (2000a) have demonstrated that the distribution of λ' is also well fit by a log-normal distribution, namely,

$$P(\lambda')d\lambda' = \frac{1}{\sqrt{2\pi\sigma_{\lambda}^2}} \exp\left(-\frac{\ln^2(\lambda'/\lambda'_0)}{2\sigma_{\lambda}^2}\right) \frac{d\lambda'}{\lambda'}, \quad (3)$$

with $\lambda'_0 = 0.035$ and $\sigma_{\lambda} = 0.5$ ¹

3. The Orbital Merger Scenario

In this section we explore the assumption that all of the orbital angular momentum of a merger is converted into the spin of the merger product. For simplicity we will consider all mergers as involving two bodies and refer to the more massive of the two progenitors as the halo and the other as the satellite. Following the merger tree algorithm (Somerville & Kolatt 1999), we neglect any mass or spin loss. We can safely neglect the internal spin of the incoming satellite because even for equal mass mergers the spin is typically only $\sim 10\%$ of the orbital angular momentum.

3.1. Encounter Parameters

Consider a satellite whose center is at a distance r from the center of the halo and moving with a

¹Note that in the log-normal distribution λ'_0 is the spin corresponding to the mean of $\ln(\lambda')$, and σ_{λ} is the standard deviation of $\ln(\lambda')$. We sometimes refer loosely to λ'_0 and σ_{λ} as the mean and standard deviation of the log-normal distribution.

velocity \vec{v} relative to the halo. Then in center of mass coordinates, the energy and angular momentum are given by

$$E_{orb} = \frac{1}{2}\mu v^2 - G \frac{M_h m_s}{r} \quad (4)$$

$$L_{orb} = \mu \vec{v} \times \vec{r} \quad (5)$$

where h and s denote the halo and satellite respectively and μ is the reduced mass, $\mu = M_h m_s / (M_h + m_s)$. We will assume that the satellite comes from outside of the halo and therefore r is at least as large as the virial radius of the halo ($r \geq R_{vir}$). For equal mass mergers ($M_h = m_s$) this implies that at some moment we can express the orbital energy in terms of the virial velocity of the halo

$$E_{orb} = m_s \left(\frac{v^2}{4} - V_{vir}^2 \right), \quad (6)$$

which makes it clear that for a given energy there is a maximum orbital angular momentum $L_{orb} \leq \mu v R_{vir}$ for the halo-satellite system. While this particular expression is only valid for equal mass mergers, the situation is similar for other encounters.

Binney & Tremaine (1987) introduce dimensionless energy and angular momentum variables (Equation 7-85):

$$\hat{E} = \frac{E_{orb}}{\frac{1}{2}\mu v_{rms}^2}; \quad \hat{L} = \frac{L_{orb}}{\mu r_e v_{rms}} \quad (7)$$

where r_e and v_{rms} are the half mass radius and rms velocity of the halo. For a halo with the NFW density profile and a concentration of ≈ 15 , $r_e = 0.3R_{vir}$ and $v_{rms} = 1.2V_{vir}$. For equal mass non-rotating spherical halos, the possible orbital parameters are shown in Figure 1. The dashed line excludes encounters that take longer than a Hubble time to merge. Adding the additional constraint that the satellite starts entirely outside of the halo, (i.e. $r \geq R_{vir}$) leaves the hatched region as the permissible range of encounter parameters. Figure 1 is only valid for equal mass mergers; in general the possible values of \hat{E} and \hat{L} will depend on M_h and m_s .

Since we do not know the probability distributions of \hat{E} or \hat{L} , we introduce a fudge factor f with which to parameterize our ignorance. Thus,

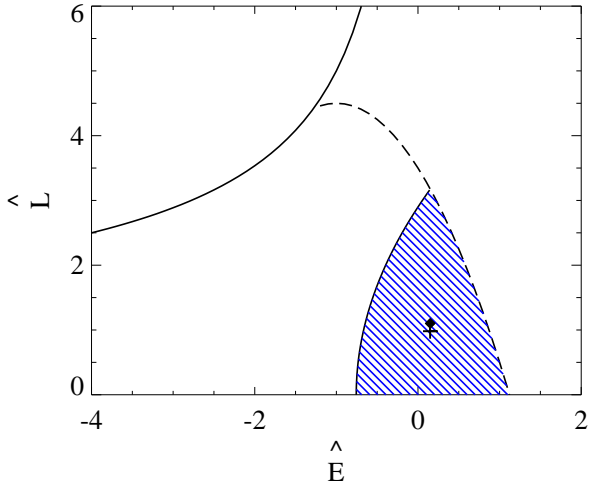


Fig. 1.— Initial encounter parameters. The parameter space of orbit energy (\hat{E}) and angular momentum (\hat{L}) for equal mass halos, following Binney & Tremaine (1987). The region above the thick solid line is excluded by definition. The region below the dashed line refers to encounters that will result in mergers within a Hubble time. The region below the thin solid line refers to halos that are separated by at least R_{vir} . The cross marks the average value of \hat{L} , and the diamond marks the value we use in our model.

we will take the orbital angular momentum of the satellite-halo system to be given by

$$L_{orb} = f \mu V_{vir} r. \quad (8)$$

If all permissible values for E_{orb} are equally likely, we would deduce from Fig. 1 that a typical value for \hat{L} is about 1, corresponding to $f \approx 0.34$. In principle, f could depend on mass and/or redshift but we will take it to be a constant and adjust it to get a good fit to the observed distribution of spin from N-body simulations; below we will find that $f = 0.38$ yields the best results. It would also be possible to determine the value of f empirically by analyzing N-body simulations (Vitvitska et al. 2001).

We generate mass accretion histories based on the formalism of Somerville & Kolatt (1999) with the slight modification introduced by Bullock, Kravtsov, & Weinberg (2000b). We produce 500 random realizations of the merger history of a halo, adopting a fixed value of f . The direction

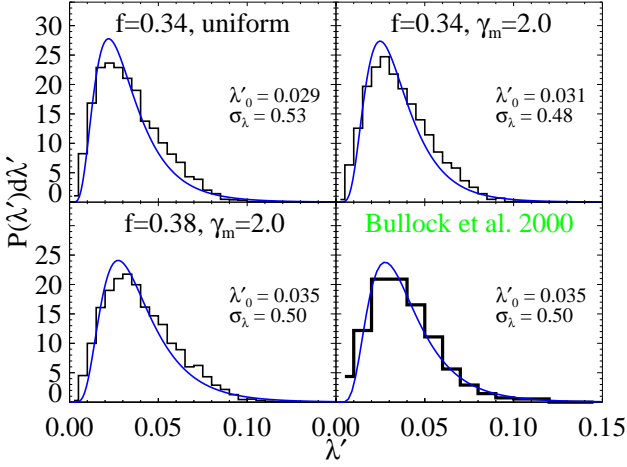


Fig. 2.— The distribution of λ' predicted by the orbital merger scenario for different values of f and γ_m , compared to the simulation data of Bullock et al. (2000a) shown in the bottom-right panel. A choice of $\gamma_m = 2.0$ and $f = 0.38$ results in a λ' distribution identical to that seen in the simulations.

of the orbital angular momentum, θ (specifically, the angle between the orbital angular momentum vector of the satellite and the spin vector of the halo), is drawn at random from a uniform or Gaussian distribution. For the uniform case, we choose $\gamma = \cos(\theta)$ from a uniform distribution between -1 and 1. For the Gaussian distribution, we choose values of γ between -1 and 1 from:

$$P(\gamma) d\gamma \propto \exp\left(-\frac{(\gamma - 1)^2}{2\gamma_m^2}\right) d\cos\gamma, \quad (9)$$

where we set the free parameter γ_m (the width of the distribution of directions) empirically. We repeat this 10 times for each history, resulting in a total of 5000 realizations. Unless specified otherwise we consider a halo at $z = 0$ of mass $5 \times 10^{11} M_\odot$ in a Λ CDM cosmology with $\Omega_m = 0.3$, $\Omega_\Lambda = 0.7$, $H_0 = 70 \text{ km s}^{-1} \text{Mpc}^{-1}$, and $\sigma_8 = 1.0$.

3.2. Results

The top-left panel of Figure 2 shows the resulting distribution of λ' for the choice $f = 0.34$ and a uniform distribution of directions θ . We note immediately that the distribution of λ' is well fit by a log-normal distribution, equation 3, with values of

λ'_0 and σ_λ fairly close to those seen in N-body simulations, shown for reference in the bottom-right panel.

We note that the value of σ_λ obtained with a fixed f and a uniform distribution of directions is somewhat larger than that seen in the simulations. This can be cured if we relax the assumption of a uniform distribution of directions, and allow for some correlation between the directions of successive mergers, as detected in N-body simulations on scales of a few hundreds of kpc (Dekel et al. 2000). We approximate this correlation by drawing the direction angle θ from a Gaussian (eqn. 9, above). As seen in the upper-right panel of Fig. 2, the choice $\gamma_m = 2.0$ reduces the value of σ_λ . The desired value of λ'_0 and σ_λ are now obtained by choosing a somewhat higher value of $f = 0.38$ (Fig. 2, bottom-left panel).

In reality, the value of f will also vary from encounter to encounter, resulting in a distribution with some scatter. This would tend to increase the scatter in λ' , which can be compensated for by a somewhat stronger correlation between the directions, namely a further decrease in the value of γ_m . For example if f is normally distributed with a standard deviation of 0.1, then to match the λ' distribution requires $\gamma_m = 1.0$ and the mean value of f to be reduced to 0.32. Here, as we don't know the form of the distribution of f we will keep things simple by assuming it to have one value. Later, our recipe could be refined by extracting from N-body simulations the detailed distributions of f and θ , and their possible dependence on mass and redshift.

4. The Tidal Torque Scenario

The standard picture of the origin of the angular momentum of DM halos, as originally introduced by Peebles (1969) and then further developed by Doroshkevich (1970) and White (1984), is formulated in the context of linear tidal torque theory. Here, material acquires its angular momentum from the large-scale tidal field while still in the linear regime. We now develop an algorithm for the generation of angular momentum in virialized halos based on the tidal torque picture and a spherical collapse model.

Linear theory (e.g. White 1984) predicts that the angular momentum of material before turn-

around, at time t , is given by:

$$J_i(t) = a(t)^2 \dot{D}(t) \epsilon_{ijk} T_{jl} I_{lk}, \quad (10)$$

where the time growth is from some fiducial initial time t_i , I_{lk} is the inertia tensor of the protohalo at t_i , and T_{jl} is the tidal (or shear) tensor at the halo center, smoothed on the halo scale. This is based on assuming the Zel'dovich approximation for the velocities inside the protohalo, and a 2nd-order Taylor expansion of the potential. Porciani & Dekel (2001) have shown that the implied standard scaling relation should be slightly modified. When applied to a collapsed shell of mass m and comoving radius q , it reads

$$dJ = g a^2(t_c) \dot{D}(t_c) \sigma(M_h) m q^2 \quad (11)$$

where $\sigma(M_h)$ is the rms density fluctuation on scale of the mass interior to the shell at t_i . The time t_c is when the shell practically stopped gaining spin. An empirical fit from simulations shows that the effective time is, on average, about one third of the spherical-model collapse time, namely slightly before turn-around (Porciani, Dekel, & Hoffman 2001a). The parameter g represents the small mis-alignment between the inertia and tidal tensors and we expect it to be ~ 0.1 (Porciani et al. 2001b).

We incorporate this into the merger trees by identifying the mass in a collapsing shell with the total mass of merging satellites (progenitor halos) and accreted mass during the same period of time. Of course the value of g will vary from halo to halo, so we assume that g is distributed normally with a mean g_0 and a standard deviation σ_g . Based on the smoothness of the tidal field across the protohalo volume, we assume that the angular momentum of each shell is in the same direction and can be added linearly. Since N-body simulations find that there is some nonlinear evolution of the spin direction at late epochs (Porciani et al. 2001b), we anticipate that g will be forced to vary with z .

We again produce 5000 values of λ' by considering 500 mass accretion histories with 10 randomly chosen values of g . At $z = 0$ in a Λ CDM cosmology, and for a halo mass of $5 \times 10^{11} M_\odot$, we find that the values $g_0 = 0.125$ and $\sigma_g = 0.44g_0$ yield a good fit to the λ' distribution in simulations (log normal with $\lambda'_0 = 0.35$ and $\sigma_\lambda = 0.50$).

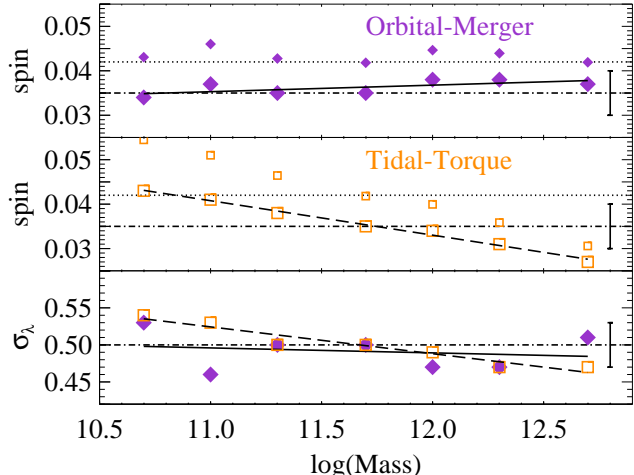


Fig. 3.— The mean and scatter of the spin at $z = 0$ as a function of halo mass, as derived from the two algorithms. The upper panel shows λ'_0 (large connected symbols) and the corresponding λ_0 (small symbols) for the orbital-merger picture with $f = 0.38$ and $\gamma_m = 2.0$. The middle panel is the analog for the tidal-torque picture with $g_0 = 0.125$ and $\sigma_g = 0.44g_0$. The bottom panel shows σ_λ for the two scenarios. The horizontal dot-dashed lines show the mass-independent values found in Bullock et al. (2001), with the corresponding errors as error bars. The dotted line is the mean value of λ from Bullock et al..

5. Independence of halo mass, cosmology and redshift

An interesting property of the distribution of the halo spin parameter, λ , as measured in cosmological N-body simulations, is that it seems to be independent of halo mass, redshift and cosmology (Lemson & Kauffmann 1999). Any model of angular momentum acquisition should therefore produce the same spin distribution irrespective of these three parameters. Indeed, our simple models seem to show this ubiquity of the λ distribution of halos, or can be adjusted to reproduce this independence by simple, physically motivated adjustments of the free parameters.

5.1. Halo Mass

Figure 3 shows the values of λ'_0 as a function of halo mass with the orbital-merger picture (upper

panel, large diamonds) and the tidal-torque scenario (middle panel, large squares). Also σ_λ as a function of halo mass is shown for both scenarios (bottom panel). We see that over the mass range most relevant for spiral galaxies ($10^{10} - 10^{12} M_\odot$) the distributions are all consistent with each other within the estimated errors (and the differences between different simulations).

For the orbital-merger model there is a slight apparent trend for λ'_0 to increase and for σ_λ to decrease as the mass increases. Note that when moving from λ' to λ this trend is expected to weaken because the halo concentration parameter is also a function of halo mass. Using the trend of average c_{vir} with halo mass found in (Bullock et al. 2000a) we can convert each λ' value to a value of λ , though this ignores the spread found in values of the c_{vir} and any possible correlations between λ' and c_{vir} . The corresponding average values of λ are also plotted (upper panel, small diamonds) in Fig. 3 and show the absence of a trend with mass. In the simulations, there are some reports of an apparent trend of λ with halo mass, in the opposite direction (Barnes & Efstathiou 1987), but this trend is weak and not seen in more recent simulations.

For the tidal-torque method different mass halos as seen in Figure 3 are all in rough agreement with the N-body results, though there is a trend towards a decrease in λ'_0 and σ_λ as mass increases. The trend in λ'_0 is in the opposite direction to that found in the orbital-merger scenario discussed above (which means that the dependence of concentration on mass implies that the trend for λ is even stronger (middle panel, small squares)).

Thus both scenarios produce values of λ' consistent with the results of simulations, though both seem to show some weak mass dependence. Whether this weak mass dependence can also be found in simulations remains to be seen. Since the trends with mass of the two scenarios are in opposite directions, detection of such a trend would tend to favor one scenario over the other.

Both trends can be removed by scaling one of the free parameters with mass. The functional forms

$$f(M_h, z) = 0.35 \left(\frac{M_h}{M_*} \right)^{-0.02} \quad (12)$$

$$g_0(M_h, z) = 0.17 \left(\frac{M_h}{M_*} \right)^{0.08}, \quad (13)$$

where M_* is the characteristic nonlinear mass (see Lacey & Cole 1993), create λ' distributions with no mass dependence (note that σ_g remains $0.44g_0$). Our reason for scaling these expressions in terms of M_* , which is a function of redshift and cosmology, will become apparent below (especially §5.3).

For the orbital merger picture the weak correction would imply that the incoming angular momentum of satellites decreases slightly as the halo's mass increases. In the tidal-torque picture we find that to remove the trend of λ' with mass requires that the misalignment between the tidal tensor and the protohalo inertia tensor is larger for more massive halos. Both of these conditions can be checked in N-body simulations.

We also observe a slight trend of σ_λ to decrease with increasing mass in both scenarios. This is a natural outcome of our modeling where the spread in λ' values arises from the spread in halo formation histories. It is unlikely for a halo to have a progenitor at a given redshift with a mass much greater than the value of M_* at that redshift. Thus the more massive a halo is the less likely it is to have assembled most of its mass long ago. This naturally leads to a narrower range of possible histories for more massive halos, and thus to the observed trend of σ_λ with halo mass. The effect is weaker in the orbital-merger algorithm where the spread in λ' is also caused by the random orientations of the incoming satellites. Future studies of simulations will be able to reveal whether such a trend exists.

5.2. Cosmology

To test the dependence on cosmology, we generate merger trees based on two other cosmological models: the original SCDM model, with an Einstein-deSitter cosmology ($\Omega_m = 1.0, \Omega_\Lambda = 0.0, H_0 = 50 \text{ km s}^{-1} \text{ Mpc}^{-1}, \sigma_8 = 0.5$), and an OCDM model, with an open cosmology ($\Omega_m = 0.3, \Omega_\Lambda = 0.0, H_0 = 70 \text{ km s}^{-1} \text{ Mpc}^{-1}, \sigma_8 = 1.0$). We compute the predicted λ' distribution in each of these cosmological models using the same fiducial values of the parameters f, γ_m, g_0 and σ_g that produced the best fit to the λ' distribution in the Λ CDM cosmology. The predictions of the orbital-merger scenario are found to be consistent

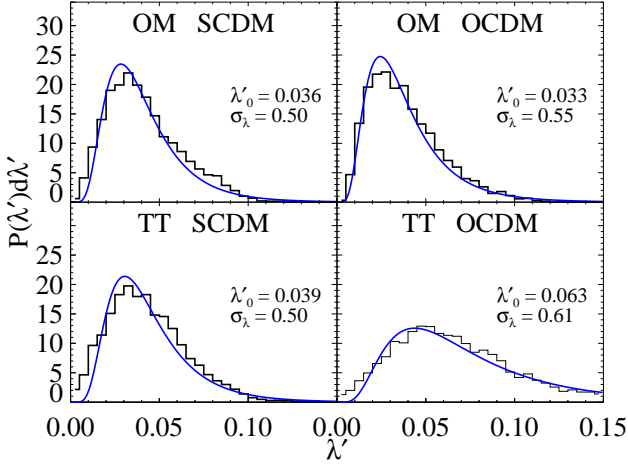


Fig. 4.— The distribution of λ' in SCDM and OCDM cosmologies predicted by the orbital-merger (OM) and tidal-torque (TT) models.

with the distribution of λ' in simulations both for SCDM and OCDM. The tidal-torque scenario recovers the distribution for the SCDM cosmology, but it predicts a somewhat higher value of λ'_0 for OCDM. These distributions slightly improve if the scaling with M_* proposed in the previous section is used. Of course the distribution of λ' in other cosmologies can be made identical to that of the Λ CDM cosmology by choosing slightly different free parameters. Again it will require higher resolution simulations to see if such trends exist or not.

5.3. Redshift

Figure 5 shows the λ' distribution as predicted by the two scenarios across the redshift range 0 to 3. We use the Λ CDM cosmology and the fiducial fixed values for the parameters f , γ_m , g_0 and σ_g .

In the orbital-merger case there is a slight increase of the mean value of λ' with redshift. As in the case of differing masses, the change in the average value of the standard spin parameter λ is weaker because concentrations evolve with redshift as $(1+z)^{-1}$. The mean value of λ is also shown in Fig. 5, and shows almost no trend with redshift. It will be interesting to see whether the trend in the average value of λ' is verified in N-body simulations.

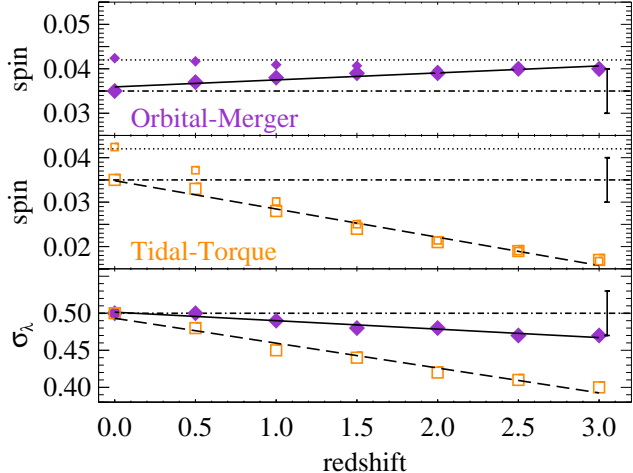


Fig. 5.— The mean and standard deviation of the spin parameters for halos of mass $5 \times 10^{11} M_\odot$ as a function of redshift, as derived by the two algorithms. The notation is as in Figure 3. Note that by redshift 1.5 concentrations become so low that λ values overlap the λ' values.

The tidal-torque method with fixed parameters produces a noticeable evolution in the mean value of λ' , dominated by the fact that shells that collapse later have had more time to gain spin via tidal torques. The evolution is even stronger when λ is considered because of the evolution of c_{vir} with redshift mentioned above. In order to keep the predicted λ' distribution constant with redshift, one needs to vary the parameter g_0 . Using the scaling of the free parameters f and g_0 introduced above in terms of M_h/M_* (equations 12 and 13), the redshift dependence of the λ' distribution is removed.

In both scenarios we see a trend for σ_λ to decrease with increasing redshift. Considering the mass of the halo over M_* it is apparent that this is the same effect as seen with variation in halo mass; halos with masses closer to or greater than M_* have less of a spread in formation history which leads to a smaller spread in their λ' distribution.

6. Merger History Dependence

Having shown that the λ distribution of halos resulting from our schemes can be made independent of cosmology, redshift or mass, in agreement

with what is found in N-body simulations, we now turn to where our scheme does predict a λ dependence — the merger history. Preliminary results from N-body simulations suggest (Gardner 2000; Wechsler et al. 2001a) that the distribution of λ is different for halos that have recently undergone a major merger. Using the same definition for a major merger (progenitor mass ratio of 1:3), we see a similar effect in our models. Figure 6 shows a significant difference between the distribution and mean value of λ' for halos that have undergone a major merger since $z = 0.5$ in both scenarios. In work in progress based on a Λ CDM simulation, Wechsler et al. find a mean value of $\log \lambda' = 0.044$ for halos identified at $z = 0$ that have had a major merger at $z < 0.5$. Those that have not had a major merger since $z = 0.5$ have a log average of 0.032, and those that have not had such a merger since $z = 2$ have a log average of 0.030. Gardner finds a similar result, a log average lambda value of 0.049 for halos that have experienced major mergers since $z = 0.5$ in an OCDM model.²

Our two different scenarios predict similar values for the mean in the log of the λ' distribution for halos with recent major mergers, 0.062 and 0.048 for the orbital-merger and tidal-torque scenarios respectively. The tidal-torque value is in good agreement with the simulations while the orbital-merger scenario gives a result $\approx 30\%$ higher than that found in simulations. If there is a situation where this algorithm might be suspect it would be the case of nearly equal mass mergers with high orbital angular momentum. In this situation our assumption that we can neglect mass loss is probably invalid, and if mass loss occurs there will inevitably also be associated loss of angular momentum. However, recent major mergers are commonly held to result in ellipticals so the effect of our overestimating λ' for these halos will have a negligible effect on disk galaxies. Our approach could be refined by treating the expected mass and angular momentum loss in a scheme similar to the

²A direct comparison between this simulation and our method is difficult because of differences in time step, halo identification, the concentration of halos, and the cosmological model. These factors make it unsurprising that we find 1120 out of 5000 halos to be recent major mergers while Gardner finds only 15 out of 1609. Our results for the fraction of halos with recent mergers are in general agreement with the simulations analyzed by Wechsler et al. (2001a), where a more consistent comparison is possible.

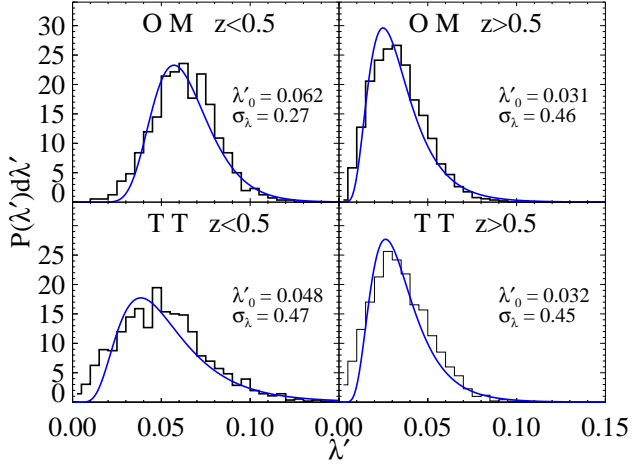


Fig. 6.— Correlation of spin and merger history. The distribution of λ' for halos that have and have not undergone major mergers since $z=0.5$ in both the orbital-merger (OM, top panels) and tidal-torque (TT, bottom panels) pictures is shown. It is surprising how similar the distributions are in these rather different pictures. We note that the log-normal distribution is not as good a fit to those halos that are recent major-merger remnants.

one we have proposed.

Mergers seem to leave a discernible mark on the halo's spin all the way back to $z = 2$. Table 1 shows the values of λ'_0 and σ_λ for the two scenarios for halos that have and have not undergone major mergers since redshifts of 0.5, 1.0 and 2.0.³ This strong connection between the merger and mass accretion history of a dark matter halo and its spin clearly has many interesting implications for galaxy formation models. This will be best investigated in detail using full semi-analytic models, but we discuss qualitatively some of the implications below.

7. Discussion

We have presented algorithms for tracing the acquisition of spin angular momentum by dark matter halos through their mass accretion or

³Like Wechsler et al. and unlike Gardner, we find that the λ' of non-mergers is different than the population as a whole. This is likely because we identify a significant fraction of halos as having undergone major merger events.

fraction of halos	Mergers				Nonmergers					
	orbital merger		tidal torque		orbital merger		tidal torque			
	λ'_0	σ_λ	λ'_0	σ_λ		λ'_0	σ_λ	λ'_0	σ_λ	
$z = 0.0$	1.0	0.035	0.50	0.035	0.50	
$z < 0.5$	0.22	0.062	0.27	0.048	0.47	0.78	0.031	0.46	0.032	0.45
$z < 1.0$	0.43	0.053	0.33	0.044	0.47	0.57	0.027	0.41	0.032	0.45
$z < 2.0$	0.68	0.044	0.41	0.039	0.48	0.32	0.023	0.41	0.028	0.44

NOTE.—The table lists value of λ'_0 and σ_λ for those halos that have suffered a major merger (3:1) since redshifts 0.5, 1.0 and 2.0 and those that have not. Also listed are the number of halos that fall into each category.

merger history. We have demonstrated that both methods reproduce the distribution of spin parameter found in N-body simulations when a small number of physically motivated free parameters are tuned appropriately.

We have proposed two such schemes, one based on the transfer of the orbital angular momentum of merging satellites to the internal spin of the halo, and another based on tidal-torque theory applied to spherical shells of collapsing material. It is interesting that these two limits of the linear and non-linear regimes produce similar results. In principle, the tidal field around a halo should influence both the halo's accretion history and the orbital angular momentum of satellites, so that in the orbital-merger model, the tidal field is still ultimately responsible for the generation of angular momentum. If we knew the details of the density field around the halo then we could calculate the orientation and magnitude of the angular momenta of the merging satellites instead of drawing them randomly in a somewhat arbitrary fashion, which is of course what an N-body simulation does.

We obtain spin distributions with respect to halo mass, redshift and differing cosmologies that are consistent within the uncertainties found in N-body simulations. We also find weak trends of the λ' distribution with mass and redshift that are in the opposite directions for the two scenarios. The dependence of concentration on mass and redshift found by Bullock et al. (2000a) creates a λ distribution without a mass or redshift trend in the orbital- merger scenario, but increases the systematic variation of λ' with redshift for the tidal-torque picture. The discovery of such a trend in

simulations would be a strong conformation of our modeling and its direction could be used to discriminate between the two scenarios.

We also find a trend for σ_λ to decrease as mass or redshift increases. This can be understood in terms of the spread in formation histories of the dark matter halo. The more massive a halo is in terms of M_h/M_* the less likely it is to have been in place for a long time as that would require progenitors with masses larger then M_* of the corresponding time. The smaller spread in formation histories in our modeling translates directly into a smaller spread in values of λ' . This also explains the trend of λ'_0 with mass and redshift found in the orbital-merger picture. As M_h/M_* increases the prevalence of recent major mergers increases which as we have shown in §6 correlates with higher spin values.

This effect should also be seen in the tidal-torque method; however, there are two other effects in this case that go in the opposite direction. Recall from equation 10 that the angular momentum gained by each shell is proportional to $\sigma(M_h)$. For larger masses $\sigma(M_h)$ is smaller and this leads to lower spin values. Likewise, at higher redshifts shells have had less time to gain angular momentum. These effects dominate over the expected increase in λ' because of late time accretion.

Because we are unsure if such trends exist in N-body simulations, we also include simple scaling relations in M_h/M_* for one of the free parameters in each scenario (f or g_0) that effectively removes the trends with mass and redshift. N-body simulations can be used to test whether g_0 and f are functions of M_h/M_* .

We have obtained the interesting prediction,

supported by preliminary recent work with N-body simulations, that there is a strong correlation between spin value and merger history. In particular, the distribution of spins for halos that have experienced recent major mergers is skewed towards higher values. This effect is discernible for major mergers at least as far back in time as $z \sim 2$. Further study of N-body simulations will test how accurately our algorithms trace this correlation between spin and merger history (Wechsler et al. 2001a).

Vitvitska et al. (2001) use N-body simulations to measure the distribution of the free parameter we term f and find its most common value to be $\approx 0.5 - 0.6$. While this is higher than the value of f we have used (0.38), they also find that to fit the λ distribution they need to assume that 25% of the angular momentum is lost during the merger event, implying that the effective value of f is very close to what we have found. Closer study of simulations will be required before we understand the details of how orbital angular momentum is transferred to spin in mergers and what dependencies are involved; however, the simple prescription we have provided here should be adequate for many applications.

These recipes can now be incorporated in semi-analytic methods that attempt to follow all the relevant physical processes of gas cooling and collapse, star formation, supernovae feedback, etc, over the formation history of galaxies. The self-consistent treatment of angular momentum acquisition that we have proposed is a significant improvement over previous work, in which spins were assigned to halos at random, from the overall distribution of λ irrespective of the halo's merger history.

We can already anticipate some of the consequences of the predicted strong dependence of spin on merger history. As an immediate example, this may explain the small spread in disk sizes found by de Jong & Lacey (2000). They argue that the standard Fall & Efstathiou (1980) picture of disk formation leads to a relation $R_d \propto \lambda L_I^\beta$ between the disk size, the spin parameter and the near-IR luminosity, implying that the spread in disk size at a given luminosity is log-normal with standard deviation $\simeq \sigma_\lambda$. However, they deduce from an observed sample of late-type spirals $\sigma_\lambda = 0.36 \pm 0.03$, which is many "sigma" away from the N-body re-

sult of $\simeq 0.5$. However, Table 1 demonstrates that considering subsamples of the halo population, divided by merger history, results in lower values of σ_λ . If we assume that late-type galaxies inhabit halos that have not experienced a major merger since a redshift of 1 or 2, then we find $0.41 < \sigma_\lambda < 0.45$, closer to the observed value. Thus, perhaps the smaller-than-predicted spread in observed disk sizes may be partially understood as the result of the special (quiescent) merger history of dark matter halos that harbor late-type galaxies. The distribution could be further narrowed by assuming that halos with very small spins also form early-type galaxies or spheroids via instability processes (Mo et al. 1998; van den Bosch 1998).

A second consequence of connecting Hubble type with merger history in this way is that the mean value of λ' for the galaxies with a quiescent history (no recent major merger) is predicted to be 10 – 15% lower than the mean of all halos. This implies a similar reduction in the prediction for the mean value of the disk scale length at a given luminosity. Whether such a reduction is problematic for the model will depend on the detailed arguments used to connect disk size to λ , and will be explored in a future work.

This research has been supported by the Israel Science Foundation grant 546/98 and by the US-Israel Binational Science Foundation grant 98-00217. AHM acknowledges the support of a Golda Meir Fellowship. We thank James Bullock, Tsafrir Kolatt, Anatoly Klypin, Andrey Kravtsov, Cristiano Porciani, Joel Primack and Risa Wechsler for stimulating discussions and help with merger trees.

REFERENCES

- Avila-Reese, V., Firmani, C., & Hernández, X. 1998, ApJ, 505, 37
- Barnes, J. & Efstathiou, G. 1987, ApJ, 319, 575
- Binney, J. & Tremaine, S. 1987, in Princeton, NJ, Princeton University Press, 1987, 747 p.
- Blumenthal, G. R., Faber, S. M., Flores, R., & Primack, J. R. 1986, ApJ, 301, 27

Bullock, J. S., Dekel, A., Kolatt, T. S., Kravtsov, A. V., A., K. A., C., P., & R., P. J. 2000a, *ApJ*, submitted, astro-ph/0011001

Bullock, J. S., Kolatt, T. S., Sigad, Y., Somerville, R. S., Kravtsov, A. V., Klypin, A. A., Primack, J. R., & Dekel, A. 2001, *MNRAS*, 321, 559

Bullock, J. S., Kravtsov, A. V., & Weinberg, D. H. 2000b, *ApJ*, 539, 517

Cole, S., Aragon-Salamanca, A., Frenk, C. S., Navarro, J. F., & Zepf, S. E. 1994, *MNRAS*, 271, 781

Cole, S., Lacey, C. G., Baugh, C. M., & Frenk, C. S. 2000, *MNRAS*, 319, 168

Dalcanton, J. J., Spergel, D. N., & Summers, F. J. 1997, *ApJ*, 482, 659

de Jong, R. S. & Lacey, C. 2000, *ApJ*, 545, 781

Dekel, A., Bullock, J. S., Porciani, C., Kravtsov, A. V., Kolatt, T. S., Kolatt, T. S., Klypin, A. A., & Primack, J. R. 2000, in *In Galaxy Disks and Disk Galaxies*, ed. S. J.G. Funes & E. Corsini, ASP Conference Series, astro-ph/0011002

Doroshkevich, A. G. 1970, *Astrofizika*, 6, 581

Fall, S. M. & Efstathiou, G. 1980, *MNRAS*, 193, 189

Firmani, C. & Avila-Reese, V. 2000, *MNRAS*, 315, 457

Flores, R., Primack, J. R., Blumenthal, G. R., & Faber, S. M. 1993, *ApJ*, 412, 443

Gardner, J. P. 2000, astro-ph/0006342

Hoyle, F. 1951, in *IAU Symp. 1: Problems of Cosmical Aerodynamics*, ed. J. M. Burgers & H. C. van de Hulst, Vol. 1 (Dayton, Ohio: Central Air Documents Office (Army-Navy-Air Force)), 195

Kauffmann, G. 1996, *MNRAS*, 281, 475

Kauffmann, G., White, S. D. M., & Guiderdoni, B. 1993, *MNRAS*, 264, 201

Lacey, C. & Cole, S. 1993, *MNRAS*, 262, 627

Lemson, G. & Kauffmann, G. 1999, *MNRAS*, 302, 111

Mestel, L. 1963, *MNRAS*, 126, 553

Mo, H. J., Mao, S., & White, S. D. M. 1998, *MNRAS*, 295, 319

Navarro, J. F., Frenk, C. S., & White, S. D. M. 1996, *ApJ*, 462, 563

Peebles, P. J. E. 1969, *ApJ*, 155, 393

Porciani, C. & Dekel, A. 2001, in preparation

Porciani, C., Dekel, A., & Hoffman, Y. 2001a, submitted to *MNRAS*, astro-ph/0105165

—. 2001b, submitted to *MNRAS*, astro-ph/0105123

Somerville, R. S. & Kolatt, T. S. 1999, *MNRAS*, 305, 1

Somerville, R. S. & Primack, J. R. 1999, *MNRAS*, 310, 1087

Somerville, R. S., Primack, J. R., & Faber, S. M. 2001, *MNRAS*, 320, 504

Steinmetz, M. & Bartelmann, M. 1995, *MNRAS*, 272, 570

van den Bosch, F. C. 1998, *ApJ*, 507, 601

—. 2000, *ApJ*, 530, 177

Vitvitska, M., Klypin, A., Kravtsov, A. V., Primack, J. R., & Wechsler, R. H. 2001, in preparation

Wechsler, R. H., Bullock, J. S., Dekel, A., Primack, J., Kravtsov, A. V., & Klypin. 2001a, in preparation

Wechsler, R. H., Bullock, J. S., Primack, J. R., Kravtsov, A. V., Klypin, A. A., & Dekel, A. 2001b, in preparation

White, S. D. M. 1984, *ApJ*, 286, 38

White, S. D. M. & Frenk, C. S. 1991, *ApJ*, 379, 52